MACKO: Sparse matrix-vector multiplication for low sparsity

Vladimír Macko 12 Vladimír Boža 1

Abstract

Sparse Matrix-Vector Multiplication (SpMV) is a fundamental operation in the inference of sparse Large Language Models (LLMs). Because existing SpMV methods perform poorly under the low and unstructured sparsity (30 - 90%) commonly observed in pruned LLMs, unstructured pruning provided only limited memory reduction and speedup. We propose MACKO-SpMV, a GPU-optimized format and kernel co-designed to reduce storage overhead while preserving compatibility with the GPU's execution model. This enables efficient SpMV for unstructured sparsity without specialized hardware units (e.g., tensor cores) or format-specific precomputation. Empirical results show that at sparsity 50%, MACKO is the first approach with significant $1.5 \times$ memory reduction and $1.2-1.5\times$ speedup over dense representation. Speedups over other SpMV baselines: $2.8-13.0 \times$ over cuSPARSE, $1.9-2.6 \times$ over Sputnik, and $2.2-2.5\times$ over DASP. Applied to Llama2-7B pruned with Wanda to sparsity 50%, it delivers $1.5 \times$ memory reduction and $1.5 \times$ faster inference at fp16 precision. Thanks to MACKO, unstructured pruning at 50% sparsity is now justified in real-world LLM workloads.

1. Introduction

Large Language Models (LLMs) (Zhang et al., 2022; Touvron et al., 2023; Dubey et al., 2024; Team et al., 2024; Jiang et al., 2024; Abdin et al., 2024) have revolutionized natural language processing and related fields. Although they are typically deployed in large data-centers, there is a growing demand for local deployment on consumer-grade GPUs, mobile devices, embedded systems, and IoT hardware.

Local inference faces major challenges due to limited hardware resources, especially memory capacity. Running the Llama2-13B model (Touvron et al., 2023), which requires

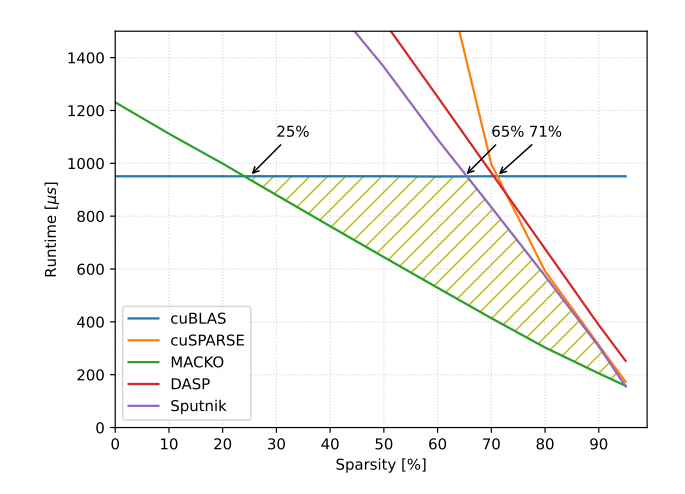


Figure 1. Sparse matrix–vector multiplication runtime. Matrix size 36864, 12288 in fp16 on an NVIDIA GeForce RTX 4090 GPU. Using MACKO, sparse computation exceeds the performance of dense at sparsity as low as 25%. Existing libraries require 2.6x fewer non-zeros to achieve the same performance. The improvement of this work is displayed as highlighted region.

about 26 GB of memory in FP16 precision, on a high-end consumer GPU such as the RTX 4090 with only 24 GB, requires compression techniques to reduce the model size and computational cost. Unstructured neural network pruning is one such promising method, allowing a large portion of weights to be removed (set to 0) with minimal degradation in model quality (Frantar & Alistarh, 2023).

The main bottleneck lies in the inefficient Sparse Matrix–Vector Multiplication (SpMV), the dominant computational kernel in local inference with sparse LLMs. SpMV is heavily used across the core layers, including QKV projections, up and down projections, and fully connected layers (Xia et al., 2023), with a typical sparsity between 50% and 90% (Lee et al., 2025). Much research has focused on improving SpMV (Greathouse & Daga, 2014; Kreutzer et al., 2014; Yan et al., 2014; Liu & Vinter, 2015; Merrill & Garland, 2016; Gale et al., 2020; Niu et al., 2021; Gómez et al., 2021; Zheng et al., 2022; Du et al., 2022; Lu & Liu, 2023; Lin et al., 2025), but all these approaches suffer from one or more of the following disadvantages: they depend on special hardware support, require extensive precomputation, or are targeted at high sparsity levels.

¹Faculty of Mathematics, Physics and Informatics Comenius University Bratislava ²GrizzlyTech. Correspondence to: Vladimir Macko <vladimir.macko@fmph.uniba.sk>.

To address these challenges, we propose MACKO-SpMV, the Mutually Aligned Compressed coordinates Kernel Optimized for Sparse Matrix Vector multiplication. MACKO introduces a novel format for representing unstructured sparse matrices based on coordinate compression with mutual alignment between coordinates and values. To achieve mutual alignment, MACKO employs strategic padding of sparse matrix elements. We show that this padding overhead is negligible in average cases and remains small and bounded even in the worst case. This enables efficient GPU implementation and as a result, state-of-the art memory reduction and speedup for 30 - 90% sparsity.

We evaluate MACKO against three state-of-the-art SpMV implementations—cusparse, dasp (Lu & Liu, 2023), and Sputnik (Gale et al., 2020), as well as a dense baseline cublas, using different consumer GPUs. For FP16 precision at 50% sparsity, MACKO is the first method that achieves a meaningful 1.2–1.5 × speedup and 1.5 × memory reduction over cublas¹. Furthermore, MACKO outperforms all baselines on all sparsity levels from 30% to 90% on all tested GPUs. These improvements directly lead to faster and more memory-efficient end-to-end LLM inference. Our key contributions are summarized as follows.

- We introduce the MACKO storage format, optimized for sparse matrices with sparsity 30–90%, and analyze its storage overhead.
- We design and implement an optimized SpMV GPU kernel and integrate it into the ML framework PyTorch.
- We conduct extensive experiments on three consumer GPUs, demonstrating that MACKO significantly outperforms existing SpMV implementations in both speed and memory efficiency.

2. Background and Related Work

This work is primarily targeted at LLM pruning, but is applicable to all models with linear layers. See Section B for a brief overview of LLM inference.

2.1. NVIDIA GPUs

NVIDIA GPUs consist of multiple *streaming multiprocessors* (SMs) and a hierarchical memory structure. The smallest unit of execution is a *thread*. The threads are grouped into *thread blocks* that form the *grid*. 32 threads within a block are grouped into a *warp* and are executed simultaneously in *single instruction multiple threads* (SIMT) mode on SM. The index of the thread within a warp is called *lane*.

The memory hierarchy consists of high latency *global memory* accessible by all threads, *shared memory* within each SM shared by threads in a thread block, and a fast but limited number of *registers* private to each thread (Guide, 2013). Access to global memory has approximately 15 times higher latency than access to shared memory, which in turn has approximately 30 higher latency than access to registers (Luo et al., 2024).

Threads can also communicate with each other in a limited way with the use of warp shuffling. Based on the shuffling pattern, this communication can be as fast as register access or as slow as shared memory access.

2.2. Quantization and Sparsification

Quantization and sparsification emerged as key model compression techniques for reducing the computational and memory demands of LLMs.

Quantization employs low-precision representations, with works introducing post-training quantization (Dettmers et al., 2022a; Frantar et al., 2022; Badri & Shaji, 2023; Tseng et al., 2024; Boža & Macko, 2024) and quantization-aware training (Wang et al., 2023; Liu et al., 2023; Du et al., 2024; Xu et al., 2024). Thanks to system-level support, such as LADDER (Wang et al., 2024), Qserve (Lin et al., 2024), MARLIN (Frantar et al., 2025), bitsandbytes (Dettmers et al., 2023; 2022b;c) and GPU support for low bit arithmetic operations (Abecassis et al., 2025), quantization is widely applicable in practice and yields predictable memory and computational improvements.

Sparsification, on the other hand, reduces the number of nonzero weights by removing the least important connections. In case the sparsity structure is unconstrained, multiple methods were able to prune a large percentage of weights without much quality degradation (LeCun et al., 1989; Frantar & Alistarh, 2023; Ma et al., 2023; Sun et al., 2023; Zhang et al., 2024; Boža, 2024; Lee et al., 2025). These methods mainly target sparsity around 50% with recent work achieving sparsity up to 90%(Lee et al., 2025). Unfortunately, they often provide no or very limited practical memory reduction or speedups.

The main bottleneck is the lack of efficient formats for storing sparse matrices and fast SpMV GPU kernels. Many works proposed methods to improve SpMV through vertical slicing (Gómez et al., 2021; Kreutzer et al., 2014), 1D tiling (Gale et al., 2020), 2D-tiling (Yan et al., 2014; Niu et al., 2021), balancing workload by reconstructing nearly evensized basic working units (Greathouse & Daga, 2014; Liu & Vinter, 2015; Merrill & Garland, 2016), utilization of hardware acceleration (Zheng et al., 2022; Lu & Liu, 2023), extensive precomputation and optimization (Du et al., 2022; Lin et al., 2025). All these approaches suffer from one or

¹cuBLAS is the strongest baseline at this sparsity level.

more of the following disadvantages: they depend on special hardware support, require extensive precomputation, or are targeted at high sparsity levels.

A common way to address the problems with sparsity is to impose constraints on the structure of non zero elements (Lagunas et al., 2021; Ma et al., 2023; Ashkboos et al., 2024). Different types of constraints were proposed and successfully utilized to achieve practical performance benefits. The most popular are: block sparsity which allows sparsity only at a level of blocks (for example, the whole 8×8 must be filled with non zeros or be completely empty) (Gray et al., 2017), and N:M sparsity which decomposes the matrix into blocks with M elements and enforces N out of those elements to be non zero (Lin et al., 2023; Castro et al., 2023). However, enforcing structural constraints often leads to an inferior model accuracy and less flexibility in model design.

2.3. System level optimizations

In practice, multiple other factors influence the final performance of the LLM serving system. Optimization of these systems focuses on restructuring computation graphs with ByteTransformer (Zhai et al., 2023) and DeepSpeed (Aminabadi et al., 2022) or refining attention mechanisms with FlashAttention (Dao et al., 2022; Dao, 2023; Shah et al., 2024). Especially relevant in a memory constrained environment are offloading methods such as those implemented in FlexGen (Sheng et al., 2023) and llama.cpp (Gerganov, 2023), which optimize memory usage by distributing model components across various hardware resources. MACKO targets weight pruning, is independent of these methods, and can be combined with them to further enhance performance.

3. Gaps and Opportunities

3.1. Bottlenecks in SpMV

To analyze the bottlenecks in SpMV, we employ the Roofline model (Williams et al., 2009) and consider the Compute Intensity (CI) of dense matrix-vector multiplication (MV) and sparse matrix-vector multiplication (SpMV) for 16-bit values compared to ops per byte (OPB) of modern GPUs.

Modern GPUs can generally perform much more operations than byte movements in a given time. This is captured by quantity *ops per byte* (OPB), defined as the ratio of peak floating point operations per second (FLOPS) to peak memory bandwidth (BW). For common GPUs OPB $\gg 1$ (80 for RTX 4090, 38 for RTX 3090, and 45 for RTX 2080).

For a matrix with R rows and C columns, the compute intensity is defined as the ratio of operations performed to the number of bytes read from and written to memory.

$$CI_{MV} = \frac{2 \cdot R \cdot C}{2 \left(R \cdot C + R + C\right)} \approx 1$$
 (1)

Given a matrix density $d=\frac{nnz}{R\cdot C}=1-sparsity$, we define effective density effd, a measure of how much memory the sparse matrix requires (storage) compared to dense representation, counting all bytes required to store the b_{val} -bit values and all bytes required to store the sparsity structure.

$$effd = \frac{storage}{R \cdot C \cdot b_{val}} \tag{2}$$

For sparse matrix-vector multiplication, the number of necessary operations decreases and the number of accessed bytes depends on the effective density *effd*.

$$CI_{SpMV} = \frac{2 \cdot d \cdot R \cdot C}{2 \left(\textit{effd} \cdot R \cdot C + R + C \right)} \approx \frac{d}{\textit{effd}} < 1$$
 (3)

Because $OPB \gg CI_{SpMV}$ and $OPB \gg CI_{MV}$, both MV and SpMV are primary limited by memory bandwidth. This is a great opportunity because improving the effective density of the sparse matrix format directly translates into less time spent on memory operations and improved performance of SpMV, as long as the computation stays compatible with the SIMT execution model and the computational overhead is sufficiently small (up to 38 operations per byte).

3.2. Analysis of storage formats

Improving the memory of the storage format directly translates into lowering the lower bound on SpMV execution time. We conduct a comparative analysis of several widely-used sparse matrix formats: CSR used by Sputnik (Gale et al., 2020) and other CUDA-core SpMM implementations, Tiled-CSL used in Flash-LLM (Xia et al., 2023), and bit-mask (Fan et al., 2025). To make the equation simpler, we disregard terms that are negligible for large matrices, such as row pointers in CSR or constant terms.

In ideal case the format would only store non zero values and effd = d which is not achievable in practice². On the other hand, dense representations provide effd = 1.

CSR32/CSR16 represents sparsity by storing column indices for each non-zero value as 32 or 16 bit integers, resulting in an effective density of:

$$effd_{CSR32} = d \cdot \frac{32 + b_{val}}{b_{val}} \tag{4}$$

$$effd_{CSR16} = d \cdot \frac{16 + b_{val}}{b_{val}} \tag{5}$$

 $^{^2}$ eff d=d is achievable only if the sparsity pattern is fully predetermined.

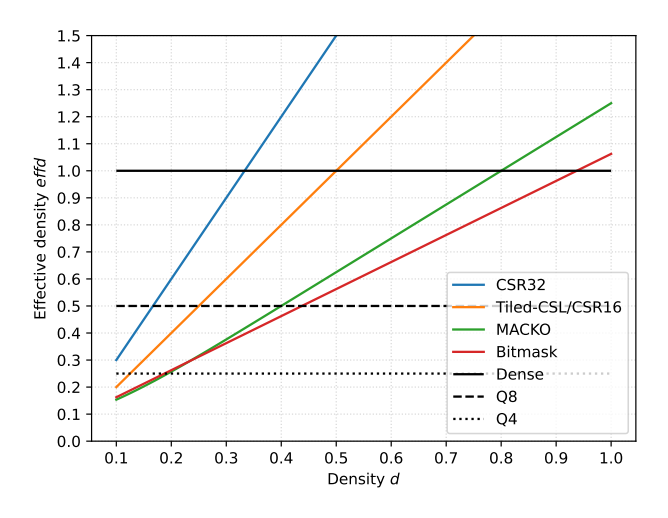


Figure 2. Effective density of different sparse matrix formats for 16-bit values. Q8 and Q4 reffer to quantization to 8 and 4 bits respectively. Expected effective density is shown for MACKO.

Tiled-CSL divides the matrix into NT tiles and stores column indices within each tile using 16 bits. For each tile, it also stores its starting offset using 32 bits.

$$effd_{Tiled-CSL} = d \cdot \frac{16 + b_{val}}{b_{val}} + \frac{32NT}{R \cdot C}$$
 (6)

The size of these tiles is usually set to at least 128×64 , making the number of tiles NT negligible compared to the total number of values $R \cdot C$ for large matrices.

Bitmask is one of the best formats in terms of effective density in a high density setting. It uses one bit per value of the original matrix to indicate whether it is zero or non-zero and an array of non-zero values. The size of the bitmask is independent of the matrix size and sparsity pattern, making it a robust choice for high-density matrices.

$$effd_{bitmask} = d + \frac{1}{b_{val}}. (7)$$

Even though this format offers great compression, it suffers from poor memory access patterns on GPUs, leading to sub-optimal performance. We are unaware of any efficient GPU SpMV implementation using bitmasking, although it has been used successfully in the matrix-matrix multiplication setting (Fan et al., 2025).

Figure 2 shows effective densities across density levels of the input matrix. MACKO has a lower effective density than CSR formats throughout the region of interest and even outperforms bitmask encoding at low density d < 0.23. Using MACKO to match the compression rate of 8-bit quantization, it is sufficient to achieve 60% model sparsity compared to 83% for CSR. This highlights the possibility of a storage format with effd as good as or better than bitmask, but compatible with the GPU execution model.

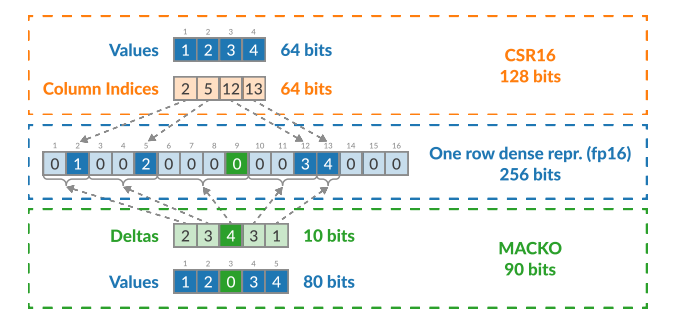


Figure 3. Example of MACKO storage format with 16 bit values and 2 bit deltas ($b_{val}=16\ b_{\Delta}=2$) compared to CSR16.

4. Design

The design of MACKO-SpMV is driven by two main goals: (1) minimize the effective density and (2) keep the SpMV algorithm compatible with the GPU parallelization model.

4.1. Compressed storage format

MACKO is inspired by the well-known CSR format. Recall that CSR represents the sparse matrix M as 3 arrays:

- values: list of non zero values of M in row major order (nnz entries, b_{val} bits per entry).
- column_indices: column index of each value (nnz entries, 16 or 32 bits per entry).
- row_pointers: indices of row beginnings in the values and column_indices arrays (R+1) entries, 32 bits per entry).

MACKO takes the column_indices for each row and compresses them using delta encoding. Then it limits the deltas to a predefined range of $[1,2^{b_{\Delta}}]$ by selectively including 0 values in the final encoding.

This padding increases the number of encoded values from the original matrix M and the length of the arrays that hold values and deltas increases from nnz to pad_nnz . We show that overhead it induces is well bounded in the worst case and almost negligible in the expected case. Mutual alignment of compressed coordinates and values enables efficient GPU kernel design and fast execution.

The resulting MACKO format looks as follows:

- values: list of non zero values of M in row major order with 0 for padding (pad_nnz) entries, b_{val} bits per entry).
- deltas: delta encoded column_indices, with fixed bit width (pad_nnz entries, b_{Δ} bits per entry).

• row_pointers: indices of row beginnings in the values and column_indices arrays (R + 1 entries, 32 bits per entry).

Figure 3 shows an example for $b_{val}=16$ and $b_{\Delta}=2$ for one row having values [1,2,3,4] with column indices [2,5,12,13] (1 based index for simplicity), MACKO inserts one 0 at columns 9. The values with padding will be [1,2,0,3,4] and the deltas [2,3,4,3,1]. MACKO trades a significant decrease in the size of deltas compared to the column_indices for a modest increase in the size of values.

Because GPU memory storage is organized into 8-bit words, we pack $\frac{8}{b_{\Delta}}$ values together using bit shifting. This limits the natural values for $b_{\Delta} \in \{1,2,4,8\}$. Although MACKO can be used with many combinations of b_{val} and b_{Δ} , we focus on $b_{val} = 16$ and $b_{\Delta} = 4$ because it has good tradeoffs between compression and generality across all density levels.

4.2. Effective density analysis

MACKO introduces overhead in the form of value padding. We analyze the impact of this padding on the effective density $effd_{MACKO}$ under 3 scenarios: the best case, the expected case, and the worst case.

Best case. If the difference between all column indices is at most 16, no value padding needs to be introduced, and only overhead comes from the deltas.

$$best_effd_{MACKO} = d\frac{b_{val} + b_{\Delta}}{b_{val}}$$
 (8)

Worst case. If all zeros in the original matrix M are in segments of length 16, they all need to be covered by padding, and we need to add $R \cdot C \cdot \frac{(1-d)}{2^b \Delta}$ new values to MACKO.

$$worst_effd_{MACKO} = \left(d + \frac{1 - d}{2^{b_{\Delta}}}\right) \frac{b_{val} + b_{\Delta}}{b_{val}}$$
 (9)

Expected case. We assume all elements of M have a uniform, independent probability d of being non zero and define $z=(1-d)^{2^b\Delta}$. The probability that a specific zero needs to be added as padding can be computed as a sum of geometric series and ends up being $d\frac{z}{1-z}$.

$$exp_effd_{MACKO} = d\left(1 + \frac{z}{1-z}\right)\frac{b_{val} + b_{\Delta}}{b_{val}}$$
 (10)

 $\frac{z}{1-z}$ starts to be noticeable only at low density d < 20%, and is dominant at very low density of d < 4%.

Thanks to this new format, **unstructured sparse matrices** match the memory footprint of dense representation for density as high as 0.78 (sparsity as low as 22%).

4.3. SplitK Matrix-Vector Multiplication

MACKO is based on a SplitK GPU algorithm for computing general matrix multiplication (GEMM) (Corporation, 2025), adapted for general matrix-vector multiplication (GEMV). The work is naturally parallelized across rows of the input matrix M, with each row M_r assigned to one warp of 32 threads. The threads in one warp collaborate to compute one value in the result vector Y_r as a product of one row M_r and vector V. The computation is parallelized across rows and across the common matrix dimension (in matrix-matrix multiplication commonly denoted as k).

For a given row r at each step i, the threads in the warp collaboratively load 32 consecutive elements from M_r and from V, one element per thread³. Then each thread $t_{\rm lane}$ computes the corresponding product $M_{r,32i+{\rm lane}}V_{32i+{\rm lane}}$ and the computation advances to the next consecutive 32 elements. After the whole row is iterated through, each thread holds part of the final product. These parts are summed using warp shuffling primitives and stored in the result matrix.

4.4. MACKO-SpMV

MACKO parallelizes the work in the same way as SplitK algorithm. Each row r of M is processed independently by a warp of 32 threads that collaboratively compute one output Y_r . MACKO is parametrized by $b_{\rm val}$, the number of bits required to store a nonzero value, and b_{Δ} , the number of bits for each delta. We present the case where $b_{\rm val}=16$ and $b_{\Delta}=4$.

MACKO computation can be split into the following parts: (1) loading deltas and values from M (2) reconstructing column indices (3) loading values from V and final computation.

We describe the algorithm for r-th row M_r of the input matrix M. The values and deltas for this row start at the index row_pointers[r] (inclusive) and end at the index row_pointers[r+1] (non inclusive).

4.4.1. Loading deltas and values from ${\it M}$

At each step, MACKO loads and processes $load_size = 8$ elements per thread. Each warp loads 128 consecutive bytes worth of deltas, which is four 8-bit words containing eight 4-bit deltas per thread. Each warp loads 512 consecutive bytes worth of values, which is eight 16-bit values per thread.

This is closely aligned with the hardware memory hierarchy and internal functions, because GPUs issue memory loads in

³Each warp typically performs one memory transaction that loads 128 bytes, resulting in one 32-bit value per thread or two 16-bit values. For efficiency, a 512-byte transaction may be used, providing four 32-bit (eight 16-bit) values per thread.

128 byte transactions. By selecting this load pattern, we are fully utilizing every memory transaction. We can make use of a similar memory loading pattern for other combinations of b_{val} and b_{Δ} .

In case of $b_{val}=16$ and $b_{\Delta}=2$, we load 128 consecutive bytes worth of deltas, which is sixteen deltas per thread. The problem is that the first 16 threads hold the deltas necessary to perform the first step, and the last 16 threads hold the deltas necessary to perform the second step. We use them across two computational steps and use warp shuffling to correctly redistribute the values to corresponding threads.

In the first step, the thread i reads the necessary deltas from thread i/2 and in the second step from 16+i/2. This value shuffling is supported on modern GPUs by <code>__shfl_sync</code> for Nvidia GPUs. It requires only the use of registers without the need to access shared or global memory and can be performed as a single instruction.

4.4.2. RECONSTRUCTING COLUMN INDICES

Each thread holds *load_size* deltas in its registers. To reconstruct the column indices, each thread needs to know the sum of all deltas stored in the previous threads. The key insight of MACKO is that this sum can be efficiently computed without any impact on memory bandwidth, which only adds computational overhead, not a memory overhead. Because matrix-vector multiplication is a memory bound, this overhead **does not** translate to runtime slowdown.

To perform the sum, each thread first computes the sum of its $load_size$ deltas $(local_sum)$ sequentially. The threads then collaborate to compute an exclusive prefix sum of the $local_sum$ values across the warp. This is done using a binary reduction tree with depth $log_2(warp_size) = 5$. At each level l of this tree, each thread holds the sum of previous 2^l threads. After Algorithm 1 is called, each thread will hold $prefix_sum$ of all deltas held by the previous threads. Finally, all threads can sequentially compute column indices corresponding to their values loaded from M.

At the end of each step, the last thread knows the sum of all deltas used in that step. We broadcast this value to all other threads in constant time using __shfl_sync(sum, 31).

4.4.3. Loading values from V and final computation

After each thread reconstructs the original column indices, it can load the corresponding value from the vector V and multiply it with the value already loaded from M. Each thread performs this for all its $load_size$ values and accumulates the sum of these products. After processing the whole row, each of the threads holds a partial dot product of the result Y_r . We sum these partial results again using warp shuffling and store the final result.

4.5. Optimization techniques

Vectorized loading is an important tool for mitigating bandwidth bottlenecks (Luitjens, 2013; Gale et al., 2020). It requires each thread in a warp to read consecutive chunks of 4, 8 or 16 bytes with addresses aligned to their respective lengths. The first consequence is that the length of the values and deltas arrays must be a multiple of 16 bytes. We solve this by padding these arrays with zeros at the end, which for non trivially large matrices adds only a negligible constant overhead. Because MACKO does not put any constraints on the number of non zeros in each row, the first load_size elements of a row may not be properly memory aligned for vectorized loading. The straightforward solution would be to pad the end of every row. We employ a more efficient technique of reverse offset memory alignment (ROMA)(Gale et al., 2020). After loading the row offset and calculating the row length, each thread decrements its row offset to the nearest vector-width-aligned address and updates the number of nonzeros that it needs to process. To maintain correctness, threads mask any values that were loaded from the previous row prior to accumulating the result in the first iteration of the main loop.

Algorithm 1 Exclusive prefix sum using warp shuffling

```
Input: current thread lane holds local_sum
Initialize prefix_sum = local_sum.
for for (i = 1; i < 32; i *= 2) do
    sync = _.shfl_up_sync(prefix_sum, i)
    if lane >= i then
        prefix_sum = prefix_sum + sync
    end if
end for
Return: prefix_sum - local_sum
```

We make use of various other well known cuda optimizations like for loop unrolling, use const and __restricted_ keywords, replacing multiplications with bit shifts where possible and removing most modulo operations. A lot of other optimizations are possible, but become GPU specific. Specifically, the use of asynchronous memory loading, cache bypassing, explicit caching of V and thread block size optimization. These optimizations often introduce new parameters that need to be specifically tuned. For the sake of this paper, we wanted to keep MACKO as general and parameter free as possible.

5. Performance Evaluation

We assess the performance of MACKO at two levels: (1) measuring pure SpMV runtime across a variety of matrix sizes, sparsity levels, and GPU models, (2) end-to-end LLM inference using MACKO-SpMV instead of linear layers.

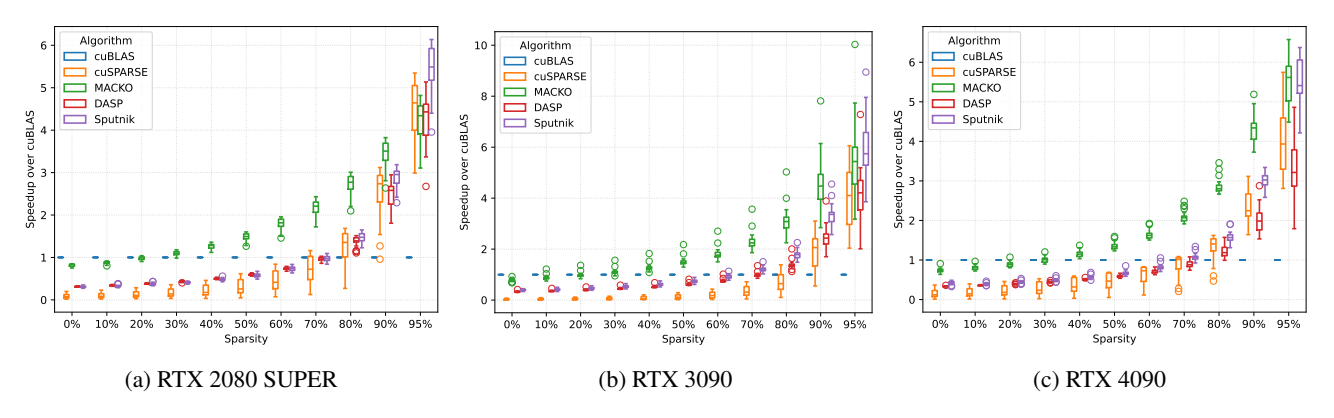


Figure 4. Relative speedup over cuBLAS across different matrix sizes.

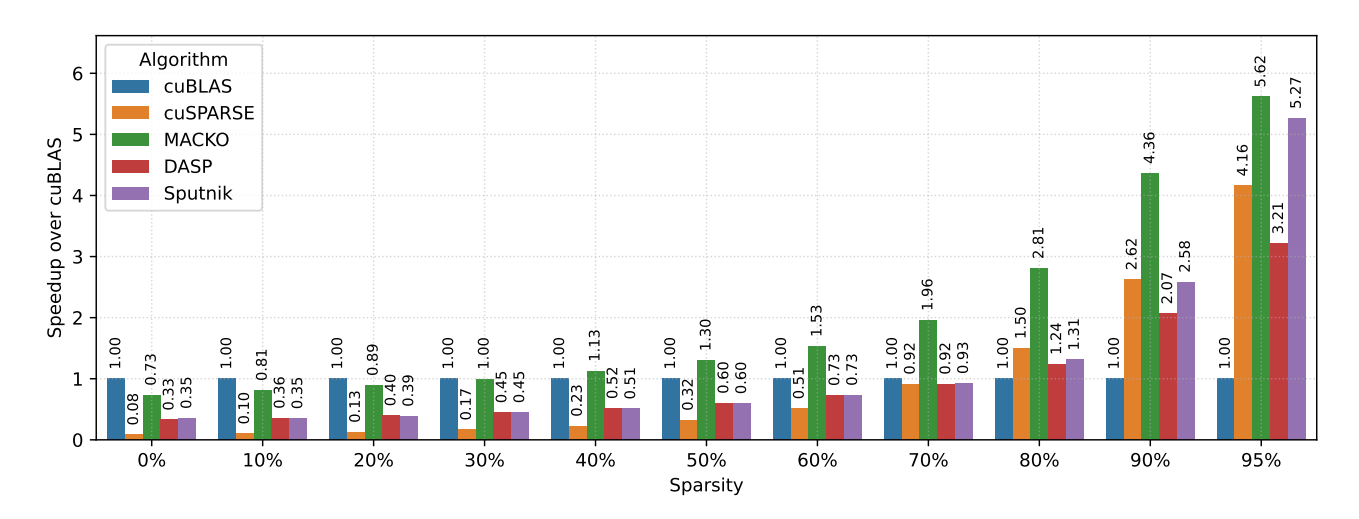


Figure 5. Speedup of MACKO relative to cuBLAS on RTX 4090 for 12288 × 12288, cuBLAS runtime 336 µs.

5.1. Runtime

Following the methodology of SpInfer-SpMM (Fan et al., 2025), we evaluate MACKO using a diverse set of matrix sizes derived from popular LLM models. These include the Llama2 series (Touvron et al., 2023), the Llama3 series (Dubey et al., 2024), the OPT-Series (Zhang et al., 2022), Qwen2 (Team et al., 2024), and the Mixtral-8×7B MoE model (Jiang et al., 2024).

We evaluate MACKO across a range of sparsity levels against (1) dense representation and cuBLAS library provided by GPU vendor (NVIDIA Corporation, 2025a) (2) cuSPARSE, sparse library provided by vendor (Naumov et al., 2010; NVIDIA Corporation, 2025b) (3) DASP, state-of-the-art SpMV library (Lu & Liu, 2023) (4) Sputnik, state-of-the-art SpMM library (Gale et al., 2020). The evaluation is conducted for the sparsity levels between 0% and 95% for completeness, even though the most interesting range for pruning is between 30% and 90%.

The SpMV experiments are performed on three different

NVIDIA GPUs: RTX 2080 SUPER (Compute Capability 7.5, 8 GB memory), RTX 3090 (Compute Capability 8.6, 24 GB memory) and RTX 4090 (Compute Capability 8.9, 24 GB memory). We measure the multiplication time in μs , averaged over 1000 runs with 100 iterations for warm starting. To model the LLM inference, we invalidate the GPU cache before every run.

Figure 4 shows performance on different GPU models. Relative speedup values are normalized by cuBLAS runtime. MACKO consistently outperforms cuSPARSE for all GPUs and all measured sparsity levels, except for the extreme sparsity of 95% where it is also outperformed by Sputnik. MACKO matches the performance of dense cuBLAS for sparsity, often as low as 20% and consistently at 30%. MACKO outperforms all baselines across all GPUs for all sparsities between 30% and 90%. This is impressive as MACKO does not introduce any tunable parameters and works out-of-the-box for all matrix sizes, sparsity levels, and GPU models, compared to the highly optimized and finetuned cuBLAS library.

Table 1. Memory requirements and generation speed of Llama2-7b pruned to different sparsity levels in dense representation compared to MACKO.

SPARSITY	DENSE	MACKO	DENSE	SPARSE
	SIZE	SIZE	SPEED	SPEED
	[GB]	[GB]	[TOKS/SEC]	[TOKS/SEC]
20%	13.59	13.77	66.55	66.36
30%	13.59	12.08	66.49	73.88
40%	13.59	10.53	66.48	85.46
50%	13.59	8.87	66.53	98.60
60%	13.59	7.14	66.51	119.27
70%	13.59	5.61	66.50	150.78
80%	13.59	4.06	66.54	193.79
90%	13.59	2.67	66.48	255.01

Figure 5 shows detailed performance on RTX 4090 for matrix size 12288×12288 . MACKO outperforms cuBLAS for all levels of sparsity above 30%, reaching $1.3\times$ speedup at 50% sparsity and $1.96\times$ at 70% sparsity, all the way to $5.62\times$ at 95% sparsity. At 95% sparsity, MACKO starts to be outperformed by other SpMV implementations, mainly Sputnik.

Using MACKO sparse computation exceeds the performance of cuBLAS at sparsity as low as 20%. Existing libraries require 2.6× fewer non-zeros to achieve the same performance.

5.2. End-to-end LLM inference

We further perform End-to-End evaluation on Llama2-7b (Touvron et al., 2023) pruned to various sparsity levels with Wanda (Sun et al., 2023) pruning algorithm in the unstructured mode. We measure the time and memory requirements to generate 100 tokens from an empty prompt. This is closely aligned with a real world use case that often decouples the prefill and decode phase (Oh et al., 2024; Patel et al., 2024; Zhong et al., 2024).

We compare the dense representation using cuBLAS multiplication with MACKO. Because MACKO is a loss-less format, for a set seed, these two models produce the exact same output up to a rounding error and minor numerical instabilities caused by non cumulative nature of float arithmetic. All experiments are run on RTX 4090.

Table 1 shows that MACKO consistently provides speedup and memory reduction for all sparsity levels above 20%. For sparsity 50% we observe $1.53\times$ memory reduction and $1.4\times$ speedup. For high sparsity levels 90%, speedup and memory reduction is somehow diminished compared to expectations based only on SpMV. This is caused by Wanda (and most other pruning algorithms) not pruning the input embedding layer nor the output embedding head. For

Llama2-7b, these layers have 262.144 MB, which is only 2% of the original model, but 10% of the model size pruned to 90% sparsity.

6. Extensions and Current Limitations

Theoretically, MACKO can achieve $1.6\times$ speedup at sparsity 50%, while our current implementation achieves $1.2-1.5\times$ speedup. The biggest possible improvement of MACKO is to introduce hardware specific optimization. Under optimal setup for specific GPU model, it is possible to achieve the same memory bandwidth as cuBLAS which will translate to $\frac{1}{effd}$ speedup.

The second possible venue for improvement is optimization for higher sparsity levels above 95%, where MACKO is outperformed by Sputnik. At these levels, the value padding becomes the dominant driver of effective density and memory bandwidth is further used by sparse access to values from vector V.

Thirdly, we hope to extend this work in the future to accommodate the combination of pruning and quantization. While MACKO shows a promising effective density even for low precisions of $b_{val}=8$ and a viable effective density for $b_{val}=4$, more optimization is needed to support efficient SpMV in these settings.

7. Conclusion

In this paper, we introduced MACKO, a novel format for representing sparse matrices at low sparsity levels accompanied by an efficient SpMV implementation for this format. We identified effective density as a primary bottleneck in SpMV and proposed a solution based on coordinate compression and strategic padding. The experimental results show that MACKO brought significant memory reduction and speedup over all SpMV baselines as well as a dense alternative for sparsity between 30% and 90%.

As seen in Figure 1, MACKO breaks the barrier of practical usability for sparsity 50%.

Future work will aim to extend these techniques to lower precisions (8-bit and 4-bit values), matrix-matrix multiplication with small batch dimensions and across even wider range of GPU models.

Software and Data

The MACKO-SpMV library is open-source and available at github.com/vlejd/macko_spmv. It includes implementation of the MACKO-SpMV cuda kernel, matrix conversion utilities, as well as integration into the torch library with enabled torch compilation.

Acknowledgements

The authors thank Vast.ai for providing easy, convenient, and reliable access to a wide variety of different GPUs. The authors thank Zhen Ning David Liu, Filip Hanzely, Marek Šuppa, and Barbora Klembarová for constructive criticism of the manuscript.

This research was supported by funding from the Slovak Research and Development Agency grant APVV-24-0045 and by grants 1/0140/25, and 1/0538/22 from the Slovak research grant agency VEGA. Part of the research results was obtained using the computational resources procured in the national project National competence centre for high performance computing (project code: 311070AKF2) funded by European Regional Development Fund, EU Structural Funds Informatization of society, Operational Program Integrated Infrastructure. We acknowledge the EuroHPC Joint Undertaking for awarding this project access to the EuroHPC supercomputer LEONARDO, hosted by CINECA (Italy) and the LEONARDO consortium through an EuroHPC Benchmark and AI Access calls.

Impact Statement

This paper presents work whose goal is to advance the field of Machine Learning. We would like to especially highlight the impact this work could have on the democratization of LLMs. Thanks to this work, running pruned LLMs on consumer hardware becomes much more feasible.

References

- Abdin, M., Aneja, J., Behl, H., Bubeck, S., Eldan, R., Gunasekar, S., Harrison, M., Hewett, R. J., Javaheripi, M., Kauffmann, P., et al. Phi-4 technical report. *arXiv* preprint arXiv:2412.08905, 2024.
- Abecassis, F., Agrusa, A., Ahn, D., Alben, J., Alborghetti, S., Andersch, M., Arayandi, S., Bjorlin, A., Blakeman, A., Briones, E., et al. Pretraining large language models with nvfp4. *arXiv preprint arXiv:2509.25149*, 2025.
- Aminabadi, R. Y., Rajbhandari, S., Awan, A. A., Li, C., Li, D., Zheng, E., Ruwase, O., Smith, S., Zhang, M., Rasley, J., et al. Deepspeed-inference: enabling efficient inference of transformer models at unprecedented scale. In SC22: International Conference for High Performance Computing, Networking, Storage and Analysis, pp. 1–15. IEEE, 2022.
- Ashkboos, S., Croci, M. L., Nascimento, M. G. d., Hoefler, T., and Hensman, J. Slicegpt: Compress large language models by deleting rows and columns. *arXiv* preprint *arXiv*:2401.15024, 2024.
- Badri, H. and Shaji, A. Half-quadratic quantization of

- large machine learning models, November 2023. URL https://mobiusml.github.io/hqq_blog/.
- Boža, V. Fast and effective weight update for pruned large language models. *arXiv preprint arXiv:2401.02938*, 2024.
- Boža, V. and Macko, V. Two sparse matrices are better than one: Sparsifying neural networks with double sparse factorization. *arXiv* preprint arXiv:2409.18850, 2024.
- Castro, R. L., Ivanov, A., Andrade, D., Ben-Nun, T., Fraguela, B. B., and Hoefler, T. Venom: A vectorized n: M format for unleashing the power of sparse tensor cores. In *Proceedings of the International Conference for High Performance Computing, Networking, Storage and Analysis*, pp. 1–14, 2023.
- Corporation, N. Efficient gemm in cuda cutlass documentation, September 2025. URL https://docs.nvidia.com/cutlass/media/docs/cpp/efficient_gemm.html. Accessed: 2025-10-27.
- Dao, T. Flashattention-2: Faster attention with better parallelism and work partitioning. *arXiv* preprint *arXiv*:2307.08691, 2023.
- Dao, T., Fu, D., Ermon, S., Rudra, A., and Ré, C. Flashattention: Fast and memory-efficient exact attention with io-awareness. *Advances in neural information processing systems*, 35:16344–16359, 2022.
- Dettmers, T., Lewis, M., Belkada, Y., and Zettlemoyer, L. Gpt3. int8 (): 8-bit matrix multiplication for transformers at scale. *Advances in neural information processing systems*, 35:30318–30332, 2022a.
- Dettmers, T., Lewis, M., Belkada, Y., and Zettlemoyer, L. Llm.int8(): 8-bit matrix multiplication for transformers at scale. *arXiv preprint arXiv:2208.07339*, 2022b.
- Dettmers, T., Lewis, M., Shleifer, S., and Zettlemoyer, L. 8-bit optimizers via block-wise quantization. *9th International Conference on Learning Representations, ICLR*, 2022c.
- Dettmers, T., Pagnoni, A., Holtzman, A., and Zettlemoyer, L. Qlora: Efficient finetuning of quantized llms. *arXiv* preprint arXiv:2305.14314, 2023.
- Du, D., Zhang, Y., Cao, S., Guo, J., Cao, T., Chu, X., and Xu, N. Bitdistiller: Unleashing the potential of sub-4-bit llms via self-distillation. *arXiv preprint arXiv:2402.10631*, 2024.
- Du, Z., Li, J., Wang, Y., Li, X., Tan, G., and Sun, N. Alphasparse: Generating high performance spmv codes directly

- from sparse matrices. In SC22: International Conference for High Performance Computing, Networking, Storage and Analysis, pp. 1–15. IEEE, 2022.
- Dubey, A., Jauhri, A., Pandey, A., Kadian, A., Al-Dahle, A., Letman, A., Mathur, A., Schelten, A., Yang, A., Fan, A., et al. The llama 3 herd of models. *arXiv e-prints*, pp. arXiv–2407, 2024.
- Fan, R., Yu, X., Dong, P., Li, Z., Gong, G., Wang, Q., Wang, W., and Chu, X. Spinfer: Leveraging low-level sparsity for efficient large language model inference on gpus. In *Proceedings of the Twentieth European Conference on Computer Systems*, pp. 243–260, 2025.
- Frantar, E. and Alistarh, D. Sparsegpt: Massive language models can be accurately pruned in one-shot. In *Interna*tional conference on machine learning, pp. 10323–10337. PMLR, 2023.
- Frantar, E., Ashkboos, S., Hoefler, T., and Alistarh, D. Gptq: Accurate post-training quantization for generative pretrained transformers. *arXiv preprint arXiv:2210.17323*, 2022.
- Frantar, E., Castro, R. L., Chen, J., Hoefler, T., and Alistarh, D. Marlin: Mixed-precision auto-regressive parallel inference on large language models. In *Proceedings of the 30th ACM SIGPLAN Annual Symposium on Principles and Practice of Parallel Programming*, pp. 239–251, 2025.
- Gale, T., Zaharia, M., Young, C., and Elsen, E. Sparse gpu kernels for deep learning. In *SC20: International Conference for High Performance Computing, Networking, Storage and Analysis*, pp. 1–14. IEEE, 2020.
- Gerganov, G. llama.cpp: Llm inference in c/c++, 2023. URL https://github.com/ggerganov/llama.cpp. GitHub repository.
- Gómez, C., Mantovani, F., Focht, E., and Casas, M. Efficiently running spmv on long vector architectures. In Proceedings of the 26th ACM SIGPLAN Symposium on Principles and Practice of Parallel Programming, pp. 292–303, 2021.
- Gray, S., Radford, A., and Kingma, D. P. Gpu kernels for block-sparse weights. *arXiv preprint arXiv:1711.09224*, 3(2):2, 2017.
- Greathouse, J. L. and Daga, M. Efficient sparse matrixvector multiplication on gpus using the csr storage format. In SC'14: Proceedings of the International Conference for High Performance Computing, Networking, Storage and Analysis, pp. 769–780. IEEE, 2014.

- Guide, D. Cuda c programming guide. *NVIDIA*, *July*, 29 (31):6, 2013.
- Jiang, A. Q., Sablayrolles, A., Roux, A., Mensch, A., Savary, B., Bamford, C., Chaplot, D. S., Casas, D. d. l., Hanna, E. B., Bressand, F., et al. Mixtral of experts. arXiv preprint arXiv:2401.04088, 2024.
- Kreutzer, M., Hager, G., Wellein, G., Fehske, H., and Bishop, A. R. A unified sparse matrix data format for efficient general sparse matrix-vector multiplication on modern processors with wide simd units. *SIAM Journal on Scientific Computing*, 36(5):C401–C423, 2014.
- Lagunas, F., Charlaix, E., Sanh, V., and Rush, A. M. Block pruning for faster transformers. *arXiv* preprint *arXiv*:2109.04838, 2021.
- LeCun, Y., Denker, J., and Solla, S. Optimal brain damage. *Advances in neural information processing systems*, 2, 1989.
- Lee, K., Jang, H., Lee, D., Alistarh, D., and Lee, N. The unseen frontier: Pushing the limits of llm sparsity with surrogate-free admm. *arXiv preprint arXiv:2510.01650*, 2025.
- Lin, B., Zheng, N., Wang, L., Cao, S., Ma, L., Zhang, Q., Zhu, Y., Cao, T., Xue, J., Yang, Y., et al. Efficient gpu kernels for n: M-sparse weights in deep learning. *Proceedings of Machine Learning and Systems*, 5:513–525, 2023.
- Lin, J., Sun, J., Lu, M., and Sun, G. Toward efficient spmv in sparse llms via block extraction and compressed storage. *arXiv preprint arXiv:2507.12205*, 2025.
- Lin, Y., Tang, H., Yang, S., Zhang, Z., Xiao, G., Gan, C., and Han, S. Qserve: W4a8kv4 quantization and system co-design for efficient llm serving. *arXiv preprint arXiv:2405.04532*, 2024.
- Liu, W. and Vinter, B. Csr5: An efficient storage format for cross-platform sparse matrix-vector multiplication. In *Proceedings of the 29th ACM on International Conference on Supercomputing*, pp. 339–350, 2015.
- Liu, Z., Oguz, B., Zhao, C., Chang, E., Stock, P., Mehdad, Y., Shi, Y., Krishnamoorthi, R., and Chandra, V. Llm-qat: Data-free quantization aware training for large language models. arXiv preprint arXiv:2305.17888, 2023.
- Lu, Y. and Liu, W. Dasp: Specific dense matrix multiply-accumulate units accelerated general sparse matrix-vector multiplication. In *Proceedings of the International Conference for High Performance Computing, Networking, Storage and Analysis*, pp. 1–14, 2023.

- Luitiens, J. Cuda pro tip: Increase performance with vectorized memory access, 2013. https://developer.nvidia.com/blog/ NVIDIA Developer Blog.
- Luo, W., Fan, R., Li, Z., Du, D., Wang, Q., and Chu, X. Benchmarking and dissecting the nvidia hopper gpu architecture. In 2024 IEEE International Parallel and Distributed Processing Symposium (IPDPS), pp. 656-667. IEEE, 2024.
- Ma, X., Fang, G., and Wang, X. Llm-pruner: On the structural pruning of large language models. Advances in neural information processing systems, 36:21702-21720, 2023.
- Merrill, D. and Garland, M. Merge-based parallel sparse matrix-vector multiplication. In SC'16: Proceedings of the International Conference for High Performance Computing, Networking, Storage and Analysis, pp. 678-689. IEEE, 2016.
- Naumov, M., Chien, L., Vandermersch, P., and Kapasi, U. Cusparse library. In GPU Technology Conference, volume 12, 2010.
- Niu, Y., Lu, Z., Dong, M., Jin, Z., Liu, W., and Tan, G. Tilespmy: A tiled algorithm for sparse matrix-vector multiplication on gpus. In 2021 IEEE International Parallel and Distributed Processing Symposium (IPDPS), pp. 68– 78. IEEE, 2021.
- NVIDIA Corporation. NVIDIA cuBLAS Library Documentation, 2025a. URL https://docs.nvidia. com/cuda/cublas/index.html. Version 12.x, Accessed: 2025-10-24.
- NVIDIA Corporation. NVIDIA cuSPARSE Library Documentation, 2025b. URL https://docs.nvidia. com/cuda/cusparse/. Accessed: 2025-10-24.
- Oh, H., Kim, K., Kim, J., Kim, S., Lee, J., Chang, D.-s., and Seo, J. Exegpt: Constraint-aware resource scheduling for llm inference. In Proceedings of the 29th ACM International Conference on Architectural Support for Programming Languages and Operating Systems, Volume 2, pp. 369-384, 2024.
- Patel, P., Choukse, E., Zhang, C., Shah, A., Goiri, Í., Maleki, S., and Bianchini, R. Splitwise: Efficient generative llm inference using phase splitting. In 2024 ACM/IEEE 51st Annual International Symposium on Computer Architecture (ISCA), pp. 118–132. IEEE, 2024.
- Shah, J., Bikshandi, G., Zhang, Y., Thakkar, V., Ramani, P., and Dao, T. Flashattention-3: Fast and accurate attention with asynchrony and low-precision. Advances in Neural Information Processing Systems, 37:68658–68685, 2024.

- Sheng, Y., Zheng, L., Yuan, B., Li, Z., Ryabinin, M., Chen, B., Liang, P., Ré, C., Stoica, I., and Zhang, C. Flexgen: High-throughput generative inference of large language cuda-pro-tip-increase-performance-with-vectodels with mesingly gput.classingly gput.classingly gput.classingly on Machine Learning, pp. 31094–31116. PMLR, 2023.
 - Sun, M., Liu, Z., Bair, A., and Kolter, J. Z. A simple and effective pruning approach for large language models. arXiv preprint arXiv:2306.11695, 2023.
 - Team, Q. et al. Qwen2 technical report. arXiv preprint arXiv:2407.10671, 2(3), 2024.
 - Touvron, H., Martin, L., Stone, K., Albert, P., Almahairi, A., Babaei, Y., Bashlykov, N., Batra, S., Bhargava, P., Bhosale, S., et al. Llama 2: Open foundation and finetuned chat models. arXiv preprint arXiv:2307.09288, 2023.
 - Tseng, A., Sun, Q., Hou, D., and De Sa, C. M. Qtip: Quantization with trellises and incoherence processing. Advances in Neural Information Processing Systems, 37: 59597-59620, 2024.
 - Vaswani, A., Shazeer, N., Parmar, N., Uszkoreit, J., Jones, L., Gomez, A. N., Kaiser, Ł., and Polosukhin, I. Attention is all you need. Advances in neural information processing systems, 30, 2017.
 - Wang, H., Ma, S., Dong, L., Huang, S., Wang, H., Ma, L., Yang, F., Wang, R., Wu, Y., and Wei, F. Bitnet: Scaling 1bit transformers for large language models. arXiv preprint arXiv:2310.11453, 2023.
 - Wang, L., Ma, L., Cao, S., Zhang, Q., Xue, J., Shi, Y., Zheng, N., Miao, Z., Yang, F., Cao, T., et al. Ladder: Enabling efficient {Low-Precision} deep learning computing through hardware-aware tensor transformation. In 18th USENIX Symposium on Operating Systems Design and Implementation (OSDI 24), pp. 307–323, 2024.
 - Williams, S., Waterman, A., and Patterson, D. Roofline: an insightful visual performance model for multicore architectures. Communications of the ACM, 52(4):65–76, 2009.
 - Xia, H., Zheng, Z., Li, Y., Zhuang, D., Zhou, Z., Qiu, X., Li, Y., Lin, W., and Song, S. L. Flash-llm: Enabling cost-effective and highly-efficient large generative model inference with unstructured sparsity. arXiv preprint arXiv:2309.10285, 2023.
 - Xu, Y., Han, X., Yang, Z., Wang, S., Zhu, Q., Liu, Z., Liu, W., and Che, W. Onebit: Towards extremely low-bit large language models. Advances in Neural Information Processing Systems, 37:66357–66382, 2024.

- Yan, S., Li, C., Zhang, Y., and Zhou, H. yaspmv: Yet another spmv framework on gpus. *Acm Sigplan Notices*, 49(8):107–118, 2014.
- Zhai, Y., Jiang, C., Wang, L., Jia, X., Zhang, S., Chen, Z., Liu, X., and Zhu, Y. Bytetransformer: A high-performance transformer boosted for variable-length inputs. In 2023 IEEE International Parallel and Distributed Processing Symposium (IPDPS), pp. 344–355. IEEE, 2023.
- Zhang, S., Roller, S., Goyal, N., Artetxe, M., Chen, M., Chen, S., Dewan, C., Diab, M., Li, X., Lin, X. V., et al. Opt: Open pre-trained transformer language models. *arXiv preprint arXiv:2205.01068*, 2022.
- Zhang, Y., Bai, H., Lin, H., Zhao, J., Hou, L., and Cannistraci, C. V. Plug-and-play: An efficient post-training pruning method for large language models. 2024.
- Zhao, W. X., Zhou, K., Li, J., Tang, T., Wang, X., Hou, Y., Min, Y., Zhang, B., Zhang, J., Dong, Z., et al. A survey of large language models. *arXiv preprint arXiv:2303.18223*, 1(2), 2023.
- Zheng, N., Lin, B., Zhang, Q., Ma, L., Yang, Y., Yang, F., Wang, Y., Yang, M., and Zhou, L. {SparTA}:{Deep-Learning} model sparsity via {Tensor-with-Sparsity-Attribute}. In *16th USENIX Symposium on Operating Systems Design and Implementation (OSDI 22)*, pp. 213–232, 2022.
- Zhong, Y., Liu, S., Chen, J., Hu, J., Zhu, Y., Liu, X., Jin, X., and Zhang, H. {DistServe}: Disaggregating prefill and decoding for goodput-optimized large language model serving. In 18th USENIX Symposium on Operating Systems Design and Implementation (OSDI 24), pp. 193–210, 2024.

A. Notation

- \bullet input vector V
- input matrix M
- output vector Y = MV
- number of non zeros in M, nnz
- number of rows and columns in M, R, C
- density of M, $d = \frac{R \cdot C}{nnz}$
- Sparsity of M, s = 1 d
- effective density effd of a storage format effd = $\frac{real_storage}{R \cdot C \cdot b_{real}}$
- number of bits to store one value in M b_{val}
- number of bits to store one delta in M_{MACKO} b_{Δ}
- max delta $2^{b_{\Delta}}$
- Compute Intensity CI
- Operations per byte ratio *OPB*
- Matrix-vector multiplication MV
- Sparse matrix-vector multiplication SpMV

B. LLM Architecture and Inference Process

LLMs are built on transformer architecture (Vaswani et al., 2017; Zhao et al., 2023), which relies on self attention mechanisms and fully connected layers. Input token embeddings are transformed into Query (Q), Key (K), and Value (V) matrices through linear projections. The attention process involves multiplying the Q and K matrices, producing attention scores that weigh the V matrix. Additionally, each transformer layer includes a Feed Forward Network (FFN) that refines token embeddings through two linear transformations with a non-linear activation in between. In case of a pruned LLM model, the Q, K and V projections from the attention part, as well as linear transformations in FFN, become sparse matrix multiplications.

LLM inference consists of two phases: the prefill and decode phases. During the prefill phase, the entire input prompt is processed in parallel via sequence of matrix-matrix multiplications, while the autoregressive decode phase generates tokens sequentially one token at a time via matrix-vector multiplications. The performance of LLMs is mainly limited by the decoding stage due to its sequential nature (Xia et al., 2023).

C. MACKO with different b_{Δ}

An interesting mode of the MACKO format is an extreme case where $b_{\Delta} = 1$. Although in the expected case this format improves memory consumption over dense representation for sparsity as low as 7% the practical improvement seems to have limited applicability.

 $b_{\Delta}=2$ is ideal for the sparsity between 15% and 45% in terms of storage. However, more research is needed for optimization of the SpMV kernel in this mode.

 $b_{\Delta}=8$ is a good alternative for very high sparsity above 95%. However, in this sparsity, the main bottleneck of SpMV becomes the scattered access to V.

D. List of matrix shapes used for benchmarking

```
[[4096,4096], [8192,8192], [8192,29568], [32000,5120], [32000,8192], [28672,8192], [5120,5120], [5120,13824], [3584,20480], [4096,11008], [13824,5120], [18944,3584], [14336,4096], [4096,14336], [8192,28672], [11008,4096], [32000,4096], [20480,3584], [3584,18944], [21504,7168], [7168,7168], [28672,7168], [7168,28672], [27648,9216], [9216,9216], [36864,9216], [9216,36864], [36864,12288], [12288,12288], [49152,12288], [12288,49152]]
```

E. SpMV runtime

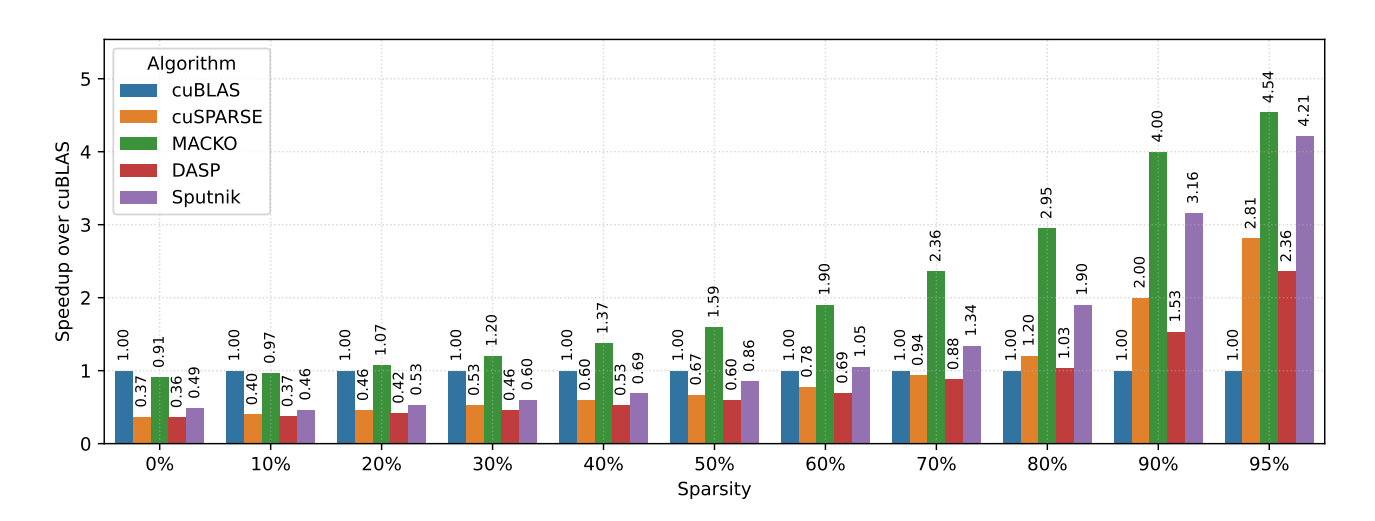


Figure 6. Speedup of MACKO relative to cuBLAS on NVIDIA GeForce RTX 4090 for 4096 × 4096, cuBLAS runtime 59 µs.

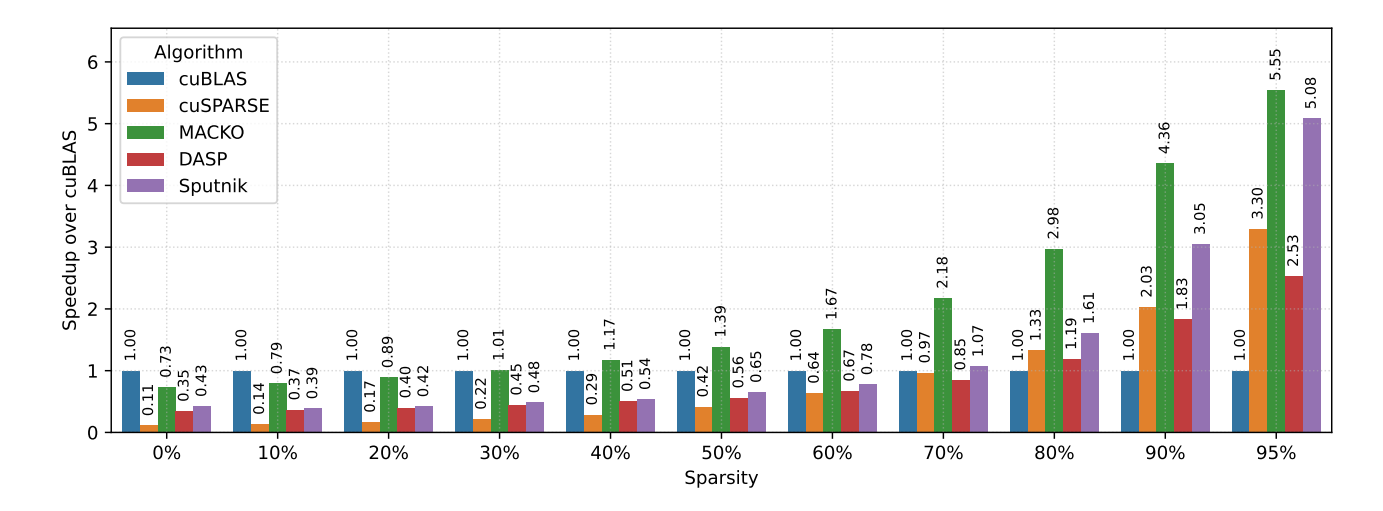


Figure 7. Speedup of MACKO relative to cuBLAS on NVIDIA GeForce RTX 4090 for 4096×11008 , cuBLAS runtime $122~\mu s$.

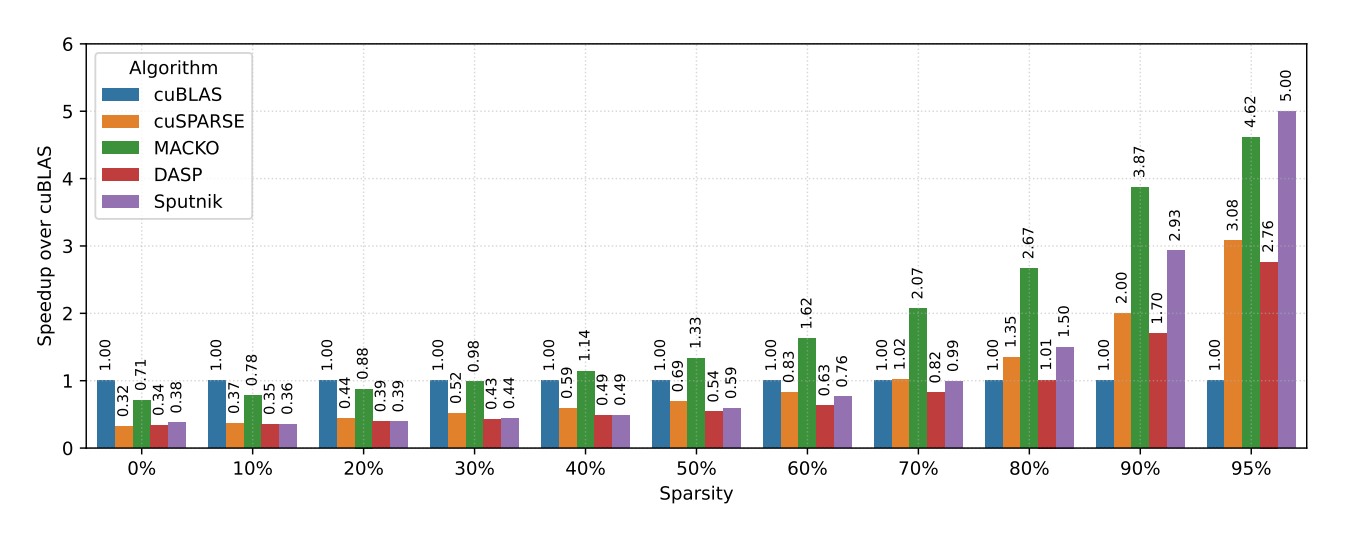


Figure 8. Speedup of MACKO relative to cuBLAS on NVIDIA GeForce RTX 4090 for 11008×4096 , cuBLAS runtime $120~\mu s$.

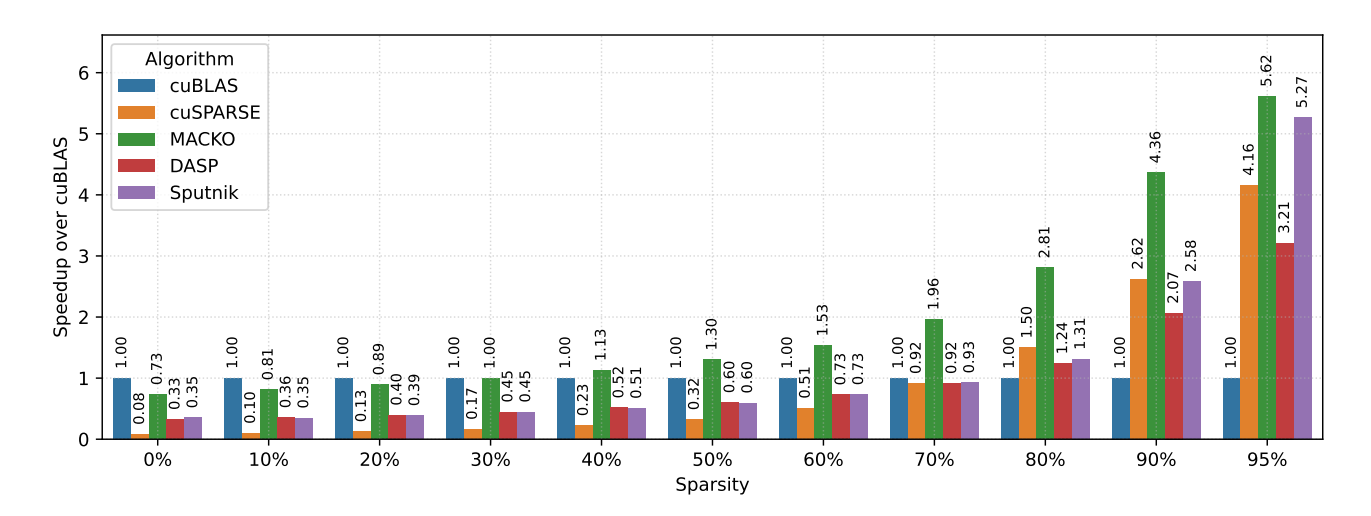


Figure 9. Speedup of MACKO relative to cuBLAS on NVIDIA GeForce RTX 4090 for 12288 \times 12288, cuBLAS runtime 336 μs .